PERGAMON

Chemical Engineering Science 54 (1999) 2141–2149

Chemical Engineering Science

Validation of the Eulerian simulated dynamic behaviour of gas–solid fluidised beds

B.G.M. van Wachem[a,b,*], J.C. Schouten[a,1], R. Krishna[b], C.M. van den Bleek[a]

[a] *Waterman Institute for Precision Chemical Engineering, Chemical Reactor Engineering Section, Delft University of Technology, Julianalaan 136, 2628 BL Delft, Netherlands*

[b] *Department of Chemical Engineering, University of Amsterdam, Nieuwe Achtergracht 166, 1018 WV Amsterdam, Netherlands*

Abstract

In this paper, a Eulerian–Eulerian CFD model for a freely bubbling gas–solid fluidised bed containing Geldart-B particles is developed for studying its dynamic characteristics. This CFD model is based on the kinetic theory of granular flow. Van Wachem et al. (1998a) Comput. Chem. Engng 22 (Suppl.), S299–S307 have shown that this model is capable of providing reasonable predictions of the *time-averaged* properties. In this paper, the *dynamic* characteristics of the gas–solids behaviour at different superficial gas velocities, at different column diameters, and at different pressures are evaluated, namely (A) the velocity of pressure and voidage waves through the bed, (B) the power of the low and high frequencies of the pressure and voidage fluctuations, (C) the reorientation of the gas–solids flow just above minimum fluidisation and the effect of elevated pressure upon this reorientation, and (D) the Kolmogorov entropy. The CFD simulation results for items (A)–(D) are compared with published experimental data and with appropriate correlations from the literature. A good agreement is found between the Eulerian–Eulerian CFD simulations of bubbling fluidised-bed dynamics, and the data from experiments in the literature. This is a strong incentive for the further development of this type of simulation models in fluidised-bed reactor design and scale-up.

Keywords: Fluidised bed; CFD; Eulerian simulations; Dynamic; Validation

1. Introduction

Fluidised beds are increasingly important in today's chemical industry; however, their hydrodynamic behaviour, and hence their scale-up, is still poorly understood. Models describing the behaviour of fluidised beds are often (semi-) empirical and have been mostly determined under laboratory conditions.

There is an increasing use of computational fluid dynamics (CFD) as an engineering tool for predicting the flow behaviour in various types of equipment on an industrial scale. Although the tools for applying single-phase flow CFD are widely available, application of multiphase CFD remains complicated from both a physical and a numerical point of view. Moreover, experimental validation of multiphase CFD calculations is still in its infancy because simulations are time-consuming, so reliable predictions of flows in large-scale equipment are not easily obtained. Van Wachem et al. (1998a) have shown that a Eulerian–Eulerian multiphase CFD model correctly predicts the time-averaged bubble properties of a gas–solid fluidised bed consisting of Geldart-B particles at various column diameters and superficial gas velocities. Besides the time-averaged properties, the dynamic characteristics of the fluidised bed's behaviour are important for choosing the appropriate conditions for stable operation and control.

The goal of the present work is to validate these dynamic characteristics of the Eulerian–Eulerian gas–solid model applied to freely bubbling fluidised beds containing Geldart-B particles, by comparing the simulated behaviour of the CFD model with trends

* Correspondence address. Waterman Institute for Precision Chemical Engineering, Chemical Reactor Engineering Section, Delft University of Technology, Julianalaan 136, 2628 BL Delft, Netherlands. Fax: 00 765 494 0805.

E-mail address: vanwachem@stm.tudelft.nl (B.G.M. van Wachem).

[1] Present address: Laboratory of Chemical Reactor Engineering, Eindhoven University of Technology, P.O. Box 513, 5600 MB Eindhoven, Netherlands.

0009-2509/99/$ – see front matter
PII: S0009-2509(98)00303-0

predicted by appropriate empirical correlations and experimental data. With this goal in mind, the operating conditions applied are the same as those were used in the development of the empirical correlations and measurements.

2. Gas–solid CFD model

The Eulerian CFD model used in this work, is based on a two-fluid model (TFM), which uses an extended Navier–Stokes equation to describe the solids phase and the gas phase so both phases are considered to be continuous and fully interpenetrating. Granular viscosities and granular pressure are derived from the kinetic theory of granular flow, which is derived from an analogy with the kinetic theory of gases (Chapman and Cowling, 1970). In this approach, thermodynamic temperature is replaced by granular flow temperature, as a measure of the fluctuating velocity of the particles. The interaction of the gas and solids phases is modelled empirically (Syamlal et al., 1993). Different TFM models have been described in the literature and are compared by Boemer et al. (1995). The most promising set of equations in the sense of fast numerical convergence and accurate physical results is used in this work.

The time-averaged equations of conservation of mass and momentum, in the Eulerian framework, are given in Table 1. The solids pressure and viscosities and the quantities needed to calculate the solids pressure and viscosities are summarized in Table 2. The interphase momentum exchange equations are given in Table 3.

Table 1
The mass and momentum balances of the Eulerian–Eulerian CFD model. The symbols are explained in the Notation (see also Van Wachem et al., 1998a)

$$\frac{\partial}{\partial t}(\varepsilon_g\rho_g) + \nabla\cdot(\varepsilon_g\rho_g\mathbf{v}_g) = 0$$

$$\frac{\partial}{\partial t}(\varepsilon_s\rho_s) + \nabla\cdot(\varepsilon_s\rho_s\mathbf{v}_s) = 0$$

$$\varepsilon_g + \varepsilon_s = 1$$

$$\frac{\partial}{\partial t}(\varepsilon_g\rho_g\mathbf{v}_g) + \nabla\cdot(\varepsilon_g\rho_g\mathbf{v}_g\mathbf{v}_g) = \nabla\cdot\bar{\bar{\tau}}_g + \varepsilon_g\rho_g\mathbf{g} + -\varepsilon_g\nabla P - \beta(\mathbf{v}_g - \mathbf{v}_s)$$

$$\frac{\partial}{\partial t}(\varepsilon_s\rho_s\mathbf{v}_s) + \nabla\cdot(\varepsilon_s\rho_s\mathbf{v}_s\mathbf{v}_s) = \nabla\cdot\bar{\bar{\tau}}_s + \varepsilon_s\rho_s\mathbf{g} + -\varepsilon_s\nabla P - \nabla P_s^* + \beta(\mathbf{v}_g - \mathbf{v}_s)$$

3. Model validation and dynamic simulation results

A pressure probe, an optic probe, or an X-ray probe can be used to determine dynamic characteristics of fluidised beds. The pressure probe measures pressure fluctuations, indirectly caused by the rising and interaction of gas bubbles, bed mass oscillation, and turbulence. Optic probes and X-ray probes measure voidage fluctuations, indirectly caused by circulating solids, gas and particle turbulence, and especially rising bubbles.

Table 2
The granular equations in the Eulerian–Eulerian CFD model are taken from Syamlal et al. (1993), Boemer et al. (1995), Ding and Gidaspow (1990), and Lun et al. (1984). An explanation of the symbols can be found in the Notation (see also Van Wachem et al., 1998a)

$$\Theta_s = \left(\frac{-(K_1\varepsilon_s + \rho_s)tr(\bar{\bar{D}}_s) + \sqrt{(K_1\varepsilon_s + \rho_s)^2 tr^2(\bar{\bar{D}}_s) + 4K_4\varepsilon_s[2K_3 tr(\bar{\bar{D}}_s^2) + K_2 tr^2(\bar{\bar{D}}_s)]}}{2\varepsilon_s K_4}\right)^2$$

$$K_1 = 2(1+e)\rho_s g_0$$

$$K_2 = \frac{4}{\sqrt[3]{\pi}} d_s\rho_s(1+e)\varepsilon_s g_0 - (2/3)K_3$$

$$K_3 = \frac{d_s\rho_s}{2}\left(\frac{\sqrt{\pi}}{3(3-e)}[1 + (2/5)(1+e)(3e-1)\varepsilon_s g_0] + \frac{8\varepsilon_s}{\sqrt[5]{\pi}} g_0(1+e)\right)$$

$$K_4 = \frac{12(1-e^2)\rho_s g_0}{d_s\sqrt{\pi}}$$

$$P_s^* = \varepsilon_s\rho_s\Theta_s(1 + 2g_0\varepsilon_s(1+e))$$

$$\lambda_s = (4/3)\varepsilon_s\rho_s d_s g_0(1+e)\sqrt{(\Theta_s/\pi)}$$

$$\mu_s = (4/5)\varepsilon_s\rho_s d_s g_0(1+e)\sqrt{(\Theta_s/\pi)} + \frac{2\sqrt[5]{\pi/96}\rho_s d_s\sqrt{\Theta_s}}{(1+e)\varepsilon_s g_0}\cdot[1 + (4/5)g_0\varepsilon_s(1+e)]^2$$

$$g_0 = (3/5)\left[1 - \left(\frac{\varepsilon_s}{\varepsilon_{s,\max}}\right)^{1/3}\right]^{-1}$$

Table 3
The interphase momentum exchange, taken from Syamlal (1993), Richardson and Zaki (1954), Dalla Valle (1948), and Garside and Al-Dibouni (1977). An explanation of the symbols can be found in the Notation (see also Van Wachem et al., 1998a)

$\beta = (3/4)C_D(\varepsilon_s\varepsilon_g\rho_g/V_r^2 d_s)\cdot\lvert\mathbf{v}_g - \mathbf{v}_s\rvert$
$C_D = 0.5\ (a - 0.06Re + \sqrt{(0.06Re)^2 + 0.12Re(2b-a) + a^2})$
$a = \varepsilon_g^{4.14}$
$b = \begin{cases} 0.8\varepsilon_g^{1.28} & \text{if } \varepsilon_s \geqslant 0.15 \\ \varepsilon_g^{2.65} & \text{if } \varepsilon_s < 0.15. \end{cases}$
$Re = (d_s\rho_g\cdot\lvert\mathbf{v}_g - \mathbf{v}_s\rvert)/\mu_g$

The processing of these signals can be done in different ways. Firstly, the velocity of the fluctuations can be studied. Secondly, the power spectral density (PSD) of the fluctuations gives information about how powerful a certain frequency in the signal is. Thirdly, fluctuations can be studied by looking at their predictability, expressed in the Kolmogorov entropy. Analysis of pressure fluctuations by Schouten and Van den Bleek (1992), Daw and Halow (1991), and Schouten et al. (1996) have revealed that fluidised beds are chaotic and low dimensional. Van den Bleek and Schouten (1993) show a reorientation occurring in fluidised beds just above minimum fluidisation.

This work validates the dynamics of the Eulerian–Eulerian gas–solid CFD model applied to fluidised beds, by (A) comparing the velocity of the pressure waves to the work of Baskakov et al. (1986) and the velocity of voidage waves to the bubble rise velocity, (B) studying the fall off of frequencies above 10 Hz, (C) comparing the predictability of the voidage and pressure fluctuations just above minimum fluidisation velocity with Van den Bleek and Schouten (1993), and (D) comparing the predictability of the voidage and pressure fluctuations at higher gas velocities with Schouten et al. (1996).

The differential and granular equations mentioned in this paper are solved with the commercial finite volume CFD package CFX4.1c from AEA Technology, Harwell, UK. The granular equations (Table 2) and the momentum transfer equations (Table 3) have been implemented in this code. The simulations are carried out in a pseudo two-dimensional square space in which there are no front and back wall effects. In this work the SIMPLE algorithm developed by Patankar (1980) is used for solving the pressure. The gas phase is treated as a compressible fluid.

For solving the difference equations obtained from the differential equations, the higher order total variation diminishing scheme min-mod is used. The time step used for the highest simulated fluidisation velocity (i.e., four times U_{mf}) is 1.0×10^{-4} s and for the lowest velocity (i.e., just above U_{mf}) twice this size is used. In this work it is found that lower fluidisation velocities require a finer mesh. The mesh chosen in this work for just above U_{mf} is $\Delta x = 7.0\times10^{-3}$ m, and for four times U_{mf} is $\Delta x = 1.0\times10^{-2}$ m.

3.1. Fluidisation conditions

The values of the model parameters used can be seen in Table 4. For the gas phase, the properties of air at ambient temperature and pressure were used. At low fluidisation velocities, simulations with two times ambient pressure were also performed. For the solids, uniform glass beads were used.

To study the reorientation phenomenon, simulations were performed with superficial gas velocities of 0.25, 0.30, 0.35, 0.40, 0.50, and 0.60 m/s in a column of 0.3 m ID. These simulations were performed at two different pressures to study the pressure effect upon the reorientation of fluidised bed hydrodynamics.

To study the PSDs of the voidage and pressure signals and to calculate the Kolmogorov entropy for comparision with the correlation of Schouten et al. (1996), superficial gas velocities of 0.50, 0.63, 0.75, 0.88, and 1.0 m/s are applied. The column diameter is varied between 0.2 and 0.4 m ID.

Since one of the goals of this work is to validate dynamic CFD simulation results with published experimental data, we would need to extract the same information from these dynamic simulations as that measured by the experimentalist. For the simulated pressure signal, pressure in a small volume, a computational mesh cell was recorded to describe an experimental pressure sensor signal as accurately as possible. Measuring the voidage or solids volume fraction by an X-ray technique, can be compared to measuring the voidage or solids volume fraction of a volume in a horizontal plane. Due to considering the fluctuations of volume fraction in a complete horizontal cross-section, global information is obtained, similar to pressure fluctuations in the bed.

Table 4
List of values of model parameters used in the simulations

Symbol	Description	Value	Comment or reference
ρ_s	Solids density	2600 kg m^{-3}	Glass beads
ρ_g	Gas density	$1.28 < \rho < 2.56$ kg m^{-3}	Used air
d_s	Particle diameter	500 μm (Geldart B type)	No size distribution
e	Coefficient of restitution	0.60	Boemer et al. (1995)
$\varepsilon_{\max}$	Maximum solids packing	0.61	Syamlal et al. (1993)
ϕ	Angle of internal friction	25°	Johnson and Jackson (1987)
U_{mf}	min. fluidisation velocity	0.25 m s^{-1}	At STP
Δt	Time step	1.0×10^{-5} s $< \Delta t < 2.0\times10^{-4}$ s	For convergence
Δx	Mesh spacing	6.0×10^{-3} m $< \Delta x < 1.0\times10^{-2}$ m	To reduce numeric diffusion
Θ_s	Granular temperature	10^{-5} m^2 s^{-2} $< \Theta_s <$ 0.1 m^2 s^{-2}	Balzer and Simonin (1993)
U_0	Superficial gas velocity	0.25 m s^{-1} $< U_0 <$ 1.0 m s^{-1}	A range is used
D_t	Column diameter	0.2 m $< D_t <$ 0.4 m	A range is used
H_t	Column height	0.6 m	Fixed value
H_s	Settled bed height	0.34 m	Fixed value

3.1.1. Velocity of pressure and voidage waves in fluidised beds

Pressure waves. It is difficult to construct a model from pressure fluctuations, predicting the complete dynamics of the fluidised bed. The dominant frequency in the pressure signal, however, is commonly reported and associated with a regular fluctuation in bed height (Roy et al., 1990). One of the models discussed by Roy et al. (1990), originally developed by Baskakov et al. (1986), describes a fluidised bed where only one bubble at a time erupts at the bed surface. The theory of this model is founded on the assumption that pressure fluctuations in the fluidised bed are similar to the oscillations of a liquid in U-shaped tubes. From this model the following can be derived:

$$t_n = \pi\sqrt{\frac{H_{mf}}{g}}, \tag{1}$$

where t_n is the natural period of oscillation of the fluidised bed. The natural period of oscillations, dominating the pressure waves, is most often experimentally assumed to coincide with the highest power in a frequency spectrum of a fluidised-bed pressure time series. This natural period can also be found by cross-correlating two pressure fluctuation signals, measured at different heights in the bed.

Fig. 1 shows an example of a simulated pressure fluctuation signal. In Fig. 2 the most dominant frequency in the pressure fluctuations obtained from CFD simulations is compared with the theory of Baskakov et al. (1986). There does not appear to be any systematic trend in dependence of this dominant frequency on the superficial gas velocity, the column diameter, or the height of the measuring probe in the fluidised bed. Prediction of the frequency of the most dominant pressure wave is in good agreement with the theory developed by Baskakov et al. (1986), especially at higher gas velocities.

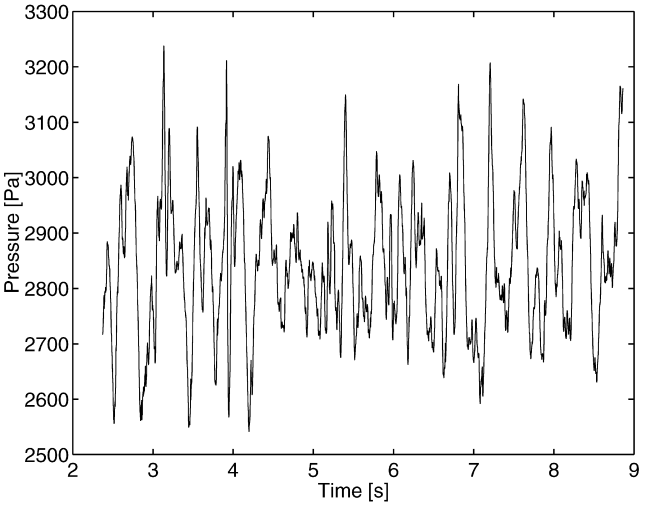

Fig. 1. Simulated pressure fluctuations in a fluidised bed, $D_t = 0.2$ m, $U_0 = 0.50$ m/s, $h = 0.1$ m. The type of particle used is given in Table 4.

Voidage waves. The natural period of oscillation is smaller for pressure fluctuations than for voidage fluctuations (the velocity of pressure waves is larger than the velocity of voidage waves). In this work, the velocity of the voidage waves is determined by cross correlating because this method is more accurate for short time series than for the natural period of oscillation.

Fig. 3 is an example of a simulated voidage signal. In Fig. 4 we compare the velocity at which the vertical component of the voidage fluctuations propagates through the column with the bubble rise velocity determined from the simulations by tracking the position of individual bubbles. It is clear from Fig. 4 that though there is a good correlation between these two velocity

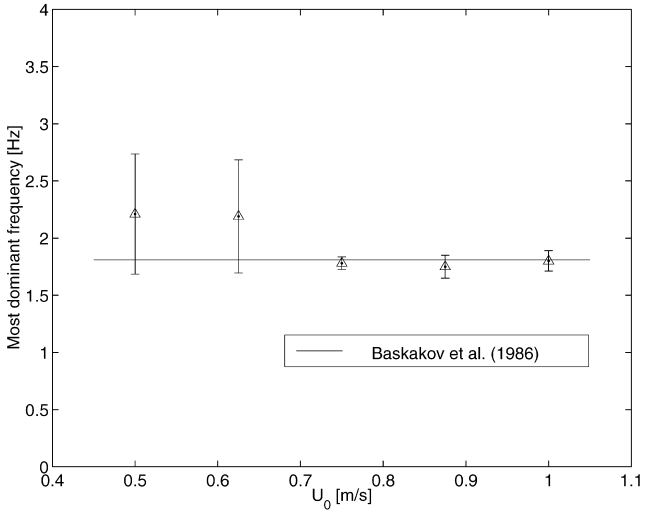

Fig. 2. The dominant frequency in the simulated pressure fluctuations as a function of the superficial gas velocity, compared to the theory of Baskakov et al. (1986). The error bars denote the spread due to data obtained at different heights in the fluidised bed and for different column diameters.

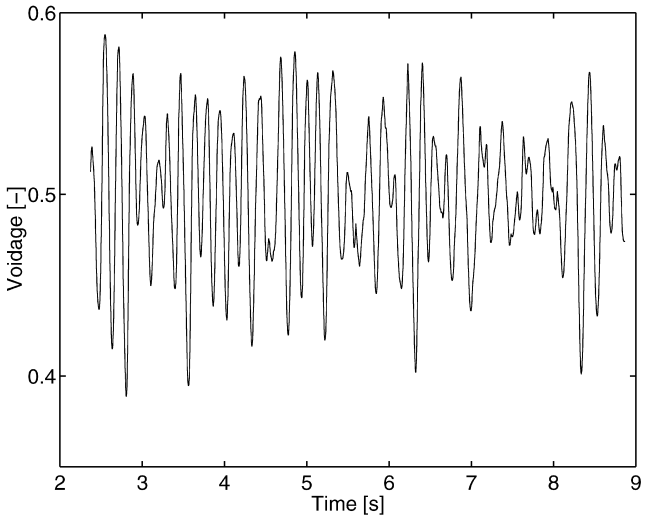

Fig. 3. Simulated voidage fluctuations in a fluidised bed, $D_t = 0.2\,\mathrm{m}$, $U_0 = 0.50\,\mathrm{m/s}$, $h = 0.1\,\mathrm{m}$.

measures, other factors such as large-scale solids circulation will influence the voidage fluctuation velocity.

3.1.2. Power of pressure and voidage waves in fluidised beds

At higher frequencies, the PSD of pressure fluctuations obtained in a fluidised bed shows a power-law decay with increasing frequency (Ding and Tam, 1994), often with a non-integer value for the slope of the power-law decay in a log–log plot. The underlying physics of this power-law decay at increasing frequency, are believed to originate from bubble coalescence and bubble formation

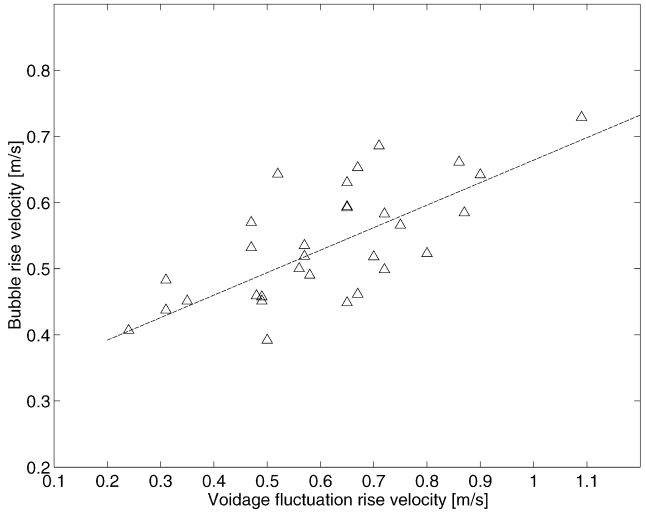

Fig. 4. The vertical voidage fluctuation velocity versus the bubble rise velocity. The line is drawn to show the trend.

(Van der Schaaf et al., 1998a). Experimentally, it has been found that the slopes of the power-law decay of the PSD of pressure fluctuations in a bubbling fluidised bed in a log–log plot is in the order of -4 (Van der Schaaf et al., 1998b).

Ding and Tam (1994) showed that the PSDs of voidage fluctuations at high frequencies also obey a power-law decay. The slope of this power-law decay in a log–log plot, however, is different from the slope of the power-law decay obtained from the PSD of pressure fluctuations in a log–log plot.

Several explanations for the power-law decay of the pressure fluctuations obtained in a fluidised bed can be found in the literature (Van der Schaaf et al., 1998b). Ding and Tam (1994) suggest that the number of possible derivatives of the measured pressure fluctuation is equal to the slope of the power-law decay in a log–log plot. This is only true, however, if the slope of the power-law decay is an integer.

Another approach to explaining power-law decay, is to study a pressure or voidage fluctuation originating from a single rising bubble in a fluidised bed: this somewhat resembles a triangular wave. The PSD of a signal consisting of triangular waves gives a very spiky power-law decay. The average slope of this power-law decay in a log–log plot, depends upon the height, width, and the number of discontinuities per period of the triangular signal. When a signal is formed from an increasing number of triangular waves, each with different characteristics, more and more spikes arise in the higher frequencies of the PSD, eventually leading to a smooth power-law behaviour, because all the valleys between two spikes are filled up by other spikes. The passage of different sizes of bubbles may somewhat resemble a measured signal with differing triangular waves, where the

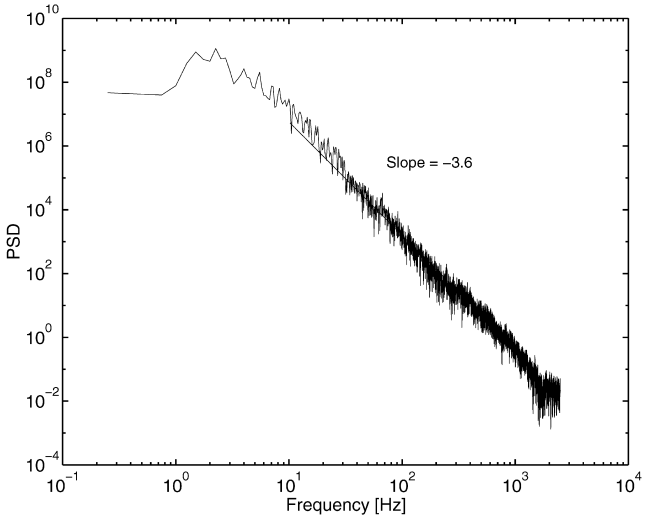

Fig. 5. Power spectral density of the simulated pressure fluctuations in a fluidised bed, $D_t = 0.2\,\text{m}$, $U_0 = 0.50\,\text{m/s}$, $h = 0.1$ m.

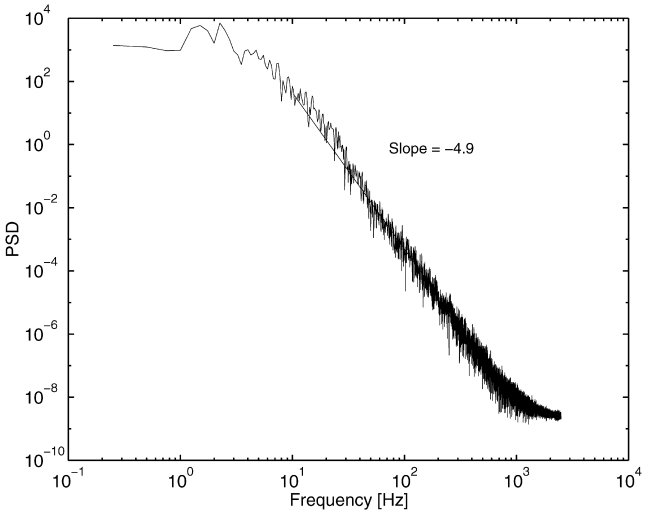

Fig. 6. Power spectral density of the simulated voidage fluctuations in a fluidised bed. $D_t = 0.2\,\text{m}$, $U_0 = 0.50\,\text{m/s}$, $h = 0.1\,\text{m}$.

amplitude (a function of bubble diameter), and the width of the triangular wave (a function of passage time) are physically coupled.

In Figs. 5 and 6, the PSDs of the simulated pressure and voidage fluctuations are shown. In Fig. 7, the slopes of the power-law decay in the log–log figures for all simulated fluidisation operating conditions are depicted. Fig. 7 shows that the operating conditions have very little influence on the slope of the power-law decay and that the values for the power-law decay of the pressure fluctuations are in good agreement with the values reported by Van der Schaaf et al. (1998b), i.e., in the order of -4. The simulated voidage fluctuations exhibit a different power-law decay than simulated pressure fluctuations, which is also shown in a simulation by Ding and Tam (1994).

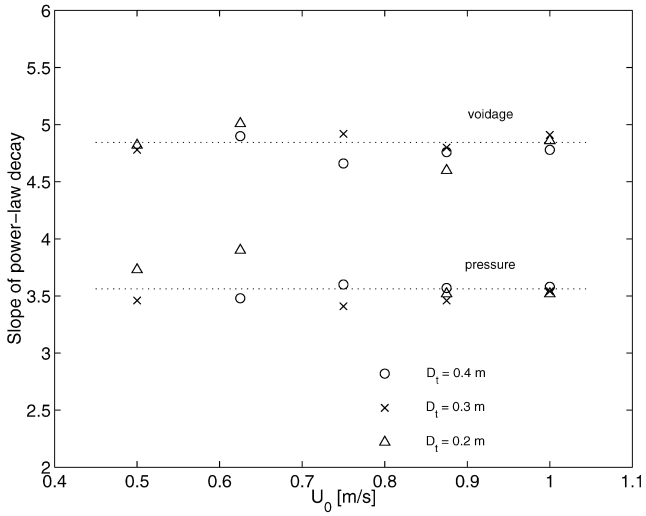

Fig. 7. The slopes of the power-law decay after about 10 Hz in the PSD figure (Figs. 5 and 6) for different column diameters, superficial gas velocities and either simulated pressure or voidage fluctuations.

3.1.3. *Reorientation effect in fluidised beds*

Van den Bleek and Schouten (1993) measured the predictability of pressure fluctuations in a gas–solid fluidised bed, expressed by the Kolmogorov entropy, as a function of the superficial gas velocity just above the minimum fluidisation velocity. It was found that between minimum fluidisation and the freely bubbling state an intermediate regime exists, where unpredictability first increases and then decreases, and then increases again. This local minimum denotes a sort of reorientation of the fluidised bed.

The particle array model (Van den Bleek and Schouten, 1993), and the fluidised bed cellular automata model (Van Wachem et al., 1998b), also show this reorientation. The underlying physics of this reorientation are not yet fully understood.

In this work, simulations are performed with Geldart-B type particles, with seven increasing superficial gas velocities. The particle type used in this work differs somewhat from the particle type used by Van den Bleek and Schouten (1993); the qualitative reorientation effect, however, is believed to be independent of particle types, and is even observed in bubble columns.

This work also presents reorientation at a higher pressure. Yates (1996) reports that elevated pressure increases the superficial gas velocity at which bubbles are formed.

The pressure and voidage time series obtained from the simulations at ambient pressure, show the same qualitative reorientation effect as that experimentally observed by Van den Bleek and Schouten (1993), as is depicted in Fig. 8. The simulations performed at two times the ambient pressure show that the valley shifts to higher gas velocities; this implies a delay in the gas velocity at which bubbles are formed, in conformity with

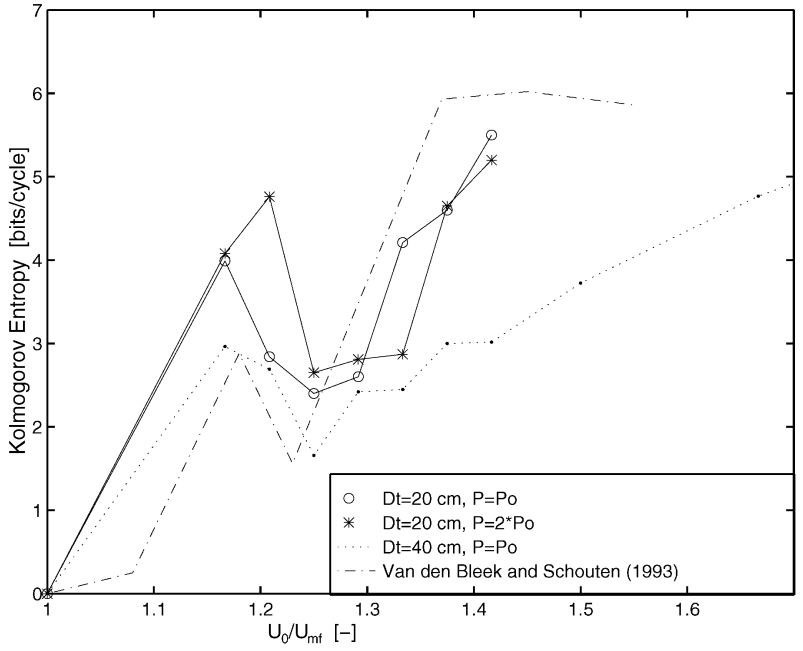

Fig. 8. The Kolmogorov entropy just above the minimum fluidisation velocity in four cases: predicted by Van den Bleek and Schouten (1993), a simulation of a 20 cm ID column at standard temperature and pressure (STP) conditions, a simulation of a 20 cm ID column at two times the standard pressure, and a simulation of a 40 cm ID column at STP conditions.

available experimental data (Yates, 1996). Fig. 8 also shows the existence of 2 transition points; the second point is where bubbling in the bed starts.

3.1.4. Chaotic behaviour of fluidised beds

The hydrodynamic behaviour of bubbling gas–solid fluidised beds can be described as chaotic (Schouten and Van den Bleek, 1992; Daw and Halow, 1991; and Schouten et al., 1996), due to rising and interacting bubbles. The chaotic characteristics of dynamic systems can be estimated from a time series of only one of the systems' characteristic variables, such as pressure or voidage fluctuations in bubbling fluidised beds. One important characteristic is the Kolmogorov entropy, which measures the rate of loss of information (expressed in bits of information per unit of time) and which quantifies the *unpredictability* of chaotic systems. Schouten et al. (1996) derived the following empirical relationship for the Kolmogorov entropy, K:

$$K(\text{bits/s}) = 10.7\left(\frac{U_0 - U_{mf}}{U_{mf}}\right)^{0.4} \frac{D_T^{1.2}}{H_s^{1.6}}. \qquad (2)$$

In this work, the Kolmogorov entropy is calculated from pressure and voidage time series produced using CFD simulations at the position of the settled bed height. The CFD simulations are performed with similar operating conditions used to establish the correlation given by Eq. (2).

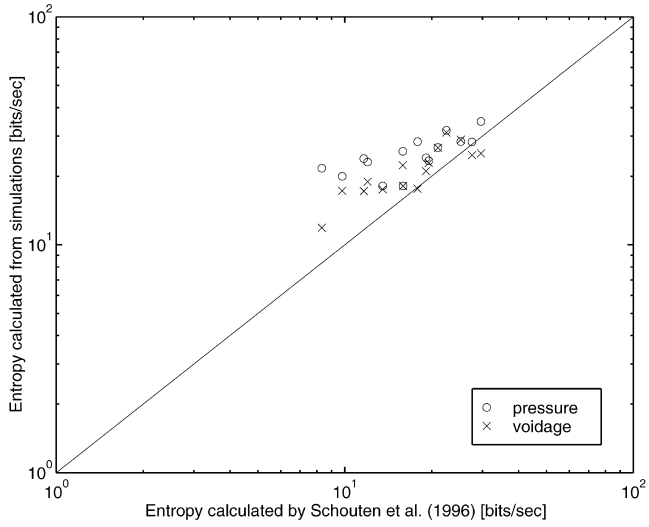

Fig. 9. The Kolmogorov entropy calculated from simulated voidage and pressure fluctuations at settled bed height, compared to Eq. (2).

The comparison between Eq. (2) and the simulations is made in Fig. 9. Although the quantitative comparison is not excellent, the simulations do reflect the behaviour of Eq. (2). Furthermore, the spread of the experimental measurements used to establish Eq. (2) is also large.

4. Conclusions

In this paper, we have shown simulations of the dynamic behaviour of laboratory-scale gas–solid fluidised beds containing Geldart-B powders. The dominant frequency of the pressure fluctuations of these simulations agrees with that in the theory of Baskakov et al. (1986). The velocity at which the voidage fluctuations propagate vertically through the column appears to correlate with the bubble rise velocity. The power-law decay characteristics of the PSD of the pressure and voidage fluctuations match those observed by Ding and Tam (1994) and Van der Schaaf et al. (1998b).

The dynamic Eulerian simulations are able to reproduce the reorientation effects in fluidised beds in the vicinity of the point at which the first bubbles are formed. Simulations with increasing pressure show that the valley in the plot of the Kolmogorov entropy versus gas velocity (Fig. 8) shifts to the right. This implies delayed bubbling, in conformity with experiments. It appears that Eulerian simulations have the intrinsic capability to portray the influence of increased system pressures.

Since we have demonstrated that Eulerian simulations are able to correctly reproduce the dynamic characteristics of laboratory-scale fluidised beds, we are reasonably confident that such simulations could be used to study the influence of column diameter and height on fluidised-bed performance. Therefore, Eulerian CFD simulations could be useful scale-up tools.

Acknowledgements

The investigations were supported in part by the Netherlands Foundation for Chemical Research (SON) with financial aid from the Netherlands Organisation for Scientific Research (NWO). This support is gratefully acknowledged.

Notation

a	defined in Table 3
b	defined in Table 3
C_D	drag coefficient
d_s	particle diameter, m
$\overline{\overline{D}}_s$	strain rate tensor, s^{-1}
D_T	column diameter, m
e	coefficient of restitution
g	gravitational constant, $m\,s^{-2}$
g_0	radial distribution function
h	height in fluidised bed, m
H_{mf}	minimum fluidisation bed height, m
H_s	settled bed height, m
H_t	column height, m
K	Kolmogorov entropy, *bits* s^{-1}
K_1, K_2, K_3, K_4	variables defined in Table 2
P	pressure, $N\,m^{-2}$
Re	Reynolds number
Δt	time step, s
t_n	natural period of oscillation, s
U_0	superficial gas velocity, $m\,s^{-1}$
U_{mf}	minimum fluidisation velocity, $m\,s^{-1}$
$\mathbf{v}$	velocity vector, $m\,s^{-1}$
V_r	ratio of terminal velocity of a group of particles to that of an isolated particle
Δx	mesh spacing, m

Greek letters

β	interphase drag constant, $kg\,m^{-3}\,s^{-1}$
ε	voidage
ϕ	angle of internal friction, $^\circ$
λ_s	bulk viscosity, Pa s
μ_s	shear viscosity, Pa s
ρ	density, $kg\,m^{-3}$
$\overline{\overline{\tau}}$	viscous stress tensor, $N\,m^{-2}$
Θ_s	granular temperature, $m^2\,s^{-2}$

Subscripts

g	gas phase
mf	minimum fluidisation
max	maximum
s	solids phase

References

Balzer, G., & Simonin, O. (1993). Extension of Eulerian gas–solid flow modelling to dense fluidized bed. In P.L. Viollet (Ed.), *Proceedings of the 5th International Symposium on Refined Flow Modelling and Turbulence Measurements*. Paris (pp. 417–424).

Baskakov, A.P., Tuponogov, V.G., & Filippovsky, N.F. (1986). A study of pressure fluctuations in a bubbling fluidized bed. *Powder Technol. 45*, 113–117.

Van den Bleek, C.M., & Schouten, J.C. (1993). Deterministic chaos: a new tool in fluidized bed design and operation. *Chem. Engng J., 53*, 75–87.

Boemer, A., Qi, H., Renz, U., Vasquez, S., & Boysan, F. (1995). Eulerian computation of fluidized bed hydrodynamics – a comparision of physical models. *Proceedings of the 13th International Conference on Fluidized Bed Combustion*. Orlando, USA. (pp. 775–786).

Chapman, S., & Cowling, T.G. (1970). *The mathematical theory of non-uniform gases*. (3rd ed.). Cambridge: Cambridge University Press.

Dalla Valle, J.M. (1948). *Micromeritics*. London: Pitman.

Daw, C.S., & Halow, J.S. (1991). Characterization of voidage and pressure signals from fluidized beds using deterministic chaos theory. In E.J. Anthony (Ed.), In *Proceedings of the 11th International Conference on Fluidized Bed Combustion*. ASME (pp. 777–786).

Ding, J., & Gidaspow, D. (1990). A bubbling fluidization model using kinetic theory of granular flow. *AIChE J*., *36*, 523–538.

Ding, J., & Tam, S. (1994). Asymptotic power spectrum analysis of chaotic behaviour in fluidized beds. *Int. J. Bifurcation Chaos*, *4*, 327–341.

Garside, J., & Al-Dibouni, M.R. (1977). Velocity–voidage relationships for fluidization and sedimentation in solid-liquid systems. *I&EC Proc. Des. Dev. 16*, 206–214.

Johnson, P.C., & Jackson, R. (1987). Frictional-collisional constitutive relations for granular materials with application to plane shearing. *J. Fluid Mech*., *176*, 67–93.

Lun, C.K.K., Savage, S.B., Jefferey, D.J., & Chepurniy, N. (1984). Kinetic theories for granular flow: Inelastic particles in Couette flow and slightly inelastic particles in a general flowfield. *J. Fluid Mech*., *140*, 223–257.

Patankar, S.V. (1980). *Numerical heat transfer and fluid flow*. USA: Hemisphere.

Richardson, J.F., & Zaki, W.N. (1954). Sedimentation and fluidisation: Part I, *Trans. Inst. Chem. Engng 32*, 35–52.

Roy, R., Davidson, J.F., & Tuponogov, V.G. (1990). The velocity of sound in fluidised beds. *Chem. Engng Sci. 45*, 3233–3245.

Schouten, J.C., & Van den Bleek, C.M. (1992). Chaotic hydrodynamics of fluidization: Consequences for scaling and modeling of fluid bed reactors. *AIChE Symp. Ser*., *289*, 780–784.

Schouten, J.C., van der Stappen, M.L.M., & van den Bleek, C.M. (1996). Scale-up of chaotic fluidized bed hydrodynamics. *Chem. Engng Sci*., *51*, 1991–2000.

Syamlal, M., Rogers, W., & O'Brien, T.J., (1993). *Mfix documentation theory guide*. DOE/METC-94/1004 (DE94000087).

Tsuji, Y., Kawaguchi, T., & Tanaka, T. (1993). Discrete particle simulation of two-dimensional fluidized bed. *Powder Technol. 77*, 79–87.

Van der Schaaf, J., Schouten, J.C., & van den Bleek, C.M. (1998a). Origin, propagation and attenuation of pressure waves in gas–solids fluidised beds. *Powder Technol. 95*, 220–233.

Van der Schaaf, J., Schouten, J.C., & van den Bleek, C.M. (1998b). Decomposition of power spectral density of pressure fluctuations in gas-solids fluidized beds. *Proceedings of the* 3*rd International Conference on Multiphase Flow*. Lyon, France.

Van Wachem, B.G.M., Schouten, J.C., Krishna, R., & van den Bleek, C.M. (1998a). Eulerian simulations of bubbling behaviour in gas–solid fluidised beds. *Comput. Chem. Engng*, *22*, (Suppl.), S299–S307.

Van Wachem, B.G.M., Bakker, A.F., Schouten, J.C., Heemels, M.W., & de Leeuw, S.W. (1998b). Simulation of fluidized beds with lattice gas cellular automata. *J. Comp. Phys*., *135*, 1–7.

Yates, J.G. (1996). Effects of temperature and pressure on gas–solid fluidization. *Chem. Engng Sci. 51*, 167–205.